

# Low-energy stripping of $\text{Kr}^+$ , $\text{Xe}^+$ , and $\text{Pb}^+$ beams in helium and nitrogen

P. Decrock,<sup>a)</sup> E. P. Kanter, and J. A. Nolen

*Physics Division, Argonne National Laboratory, Argonne, Illinois 60439*

(Received 23 January 1997; accepted for publication 19 February 1997)

Stripping efficiencies for  $\text{Kr}^+$ ,  $\text{Xe}^+$ , and  $\text{Pb}^+$  beams in helium and nitrogen gas targets have been measured at energies varying between 0.8 and 2.0 MeV. The stripping yields were determined for different target densities, ranging from single-collision conditions to equilibrium. Based on these results, approximate predictions of the equilibrium charge state distributions for low velocity ( $v/c=0.0040-0.0060$ ) heavy ions with  $28 < Z < 92$  in collisions with helium atoms are made. Furthermore, measurements of the small-angle scattering of these heavy ion beams in collisions with dilute helium and nitrogen gases are reported. The presented results are important in view of a proposed postacceleration scheme for low-energy radioactive ion beams using a linac. These data show that helium generally produces higher yields of  $2^+$  and  $3^+$  ions and that the optimal choice of gas thickness for the proposed application is somewhat less than that required for equilibrium.

© 1997 American Institute of Physics. [S0034-6748(97)02106-0]

## I. INTRODUCTION

A novel scheme for producing energetic radioactive nuclear beams, has recently been suggested.<sup>1</sup> The scheme consists of producing low-energy  $1^+$  isotope separator on-line (ISOL) beams, which will be postaccelerated using two normally conducting radio frequency quadrupoles and two superconducting linear accelerators (maximum total energy  $\approx 6-15$  MeV/nucleon).<sup>1-3</sup> Two stripping stages are foreseen in the acceleration scheme: a first stripping at about 8 keV/nucleon using a windowless gas target and a second stripping at about 0.5 MeV/nucleon using a foil target.<sup>1</sup> With this acceleration scheme, a low velocity gas stripping is necessary from  $1^+$  to  $2^+$  and from  $1^+$  to  $3^+$  for masses larger than 70 and 140, respectively.<sup>1-3</sup> Eventually, for possible applications involving masses higher than 210, gas stripping from  $1^+$  to  $4^+$  would be needed for these special cases. An overall gain in radioactive beam intensity is expected with this new acceleration scheme when compared with the Iso-Spin Laboratory benchmark facility proposal<sup>4</sup> where the first stripping takes place at higher energies ( $\approx 150$  keV/u). Besides a high stripping efficiency, small multiple scattering of the beam is required in order to maintain a high-quality secondary beam. Unfortunately, few stripping data have been reported at these very low velocities. For these reasons, we have measured stripping yields of Kr, Xe, and Pb beams in gases at various target densities, going from nonequilibrium to equilibrium charge state distributions. In addition, stripping yields for  $\text{N}^+$  beams in helium and nitrogen have been measured in order to examine the experimental method and to determine the effective target thickness. A prediction of the equilibrium charge state distribution for low velocity heavy ions with  $28 < Z < 92$  is discussed as well. Furthermore, the angular broadening of the beams due to multiple scattering in the gas target has been measured for various helium and nitrogen target thicknesses.

## II. EXPERIMENTAL SETUP

The beams were produced by the 5-MV Dynamitron accelerator in the ANL Physics Division. The  $1^+$  beams were first analyzed by two bending magnets and then further collimated using 1 mm circular apertures separated by 10 m along the beam line, yielding a maximum angular divergence of  $\pm 0.1$  mrad. This beam was then passed through a differentially pumped windowless gas cell. The 10 cm long internal chamber had an entrance aperture of 2.0 mm in diameter and a vertical exit aperture of 1.6 mm wide and 5.0 mm high. The pressure in the cell, which was measured with a Pirani gauge, could be varied between  $1.0 \times 10^{-3}$  and  $1.0 \times 10^{-1}$  Torr. This windowless gas target is described in Ref. 5. The different charge states were analyzed using a 70 cm long parallel plate deflector beginning  $\sim 50$  cm downstream of the target exit. The charge state fractions were measured with a movable silicon particle detector, positioned 5.5 m downstream of the gas target. For the measurements of the charge state fractions, a rectangular slit with a width of 10 mm and a height of 22 mm was positioned in front of the silicon detector. By installing a narrower rectangular slit (width  $\approx 1.2$  mm), a scan of the beam profile with an angular resolution of  $\approx 0.2$  mrad could be performed, and information about multiple scattering in the gas target was also obtained.

## III. RESULTS AND DISCUSSION

### A. Charge state fractions

#### 1. Nitrogen results

The experimental method was first examined by using a 2 MeV  $\text{N}^+$  beam and helium and nitrogen as the stripper gases. Figure 1 shows the results of the charge state fractions obtained with a 2 MeV  $\text{N}^+$  beam as a function of the He and  $\text{N}_2$  densities. While the initial  $1^+$  charge state fraction is depopulated with increasing target density, the other charge state fractions generally increase until an equilibrium charge state distribution is reached, i.e., when the charge state fractions do not change when the target density is further in-

<sup>a)</sup>Electronic mail: decrock@anlphy.phy.anl.gov

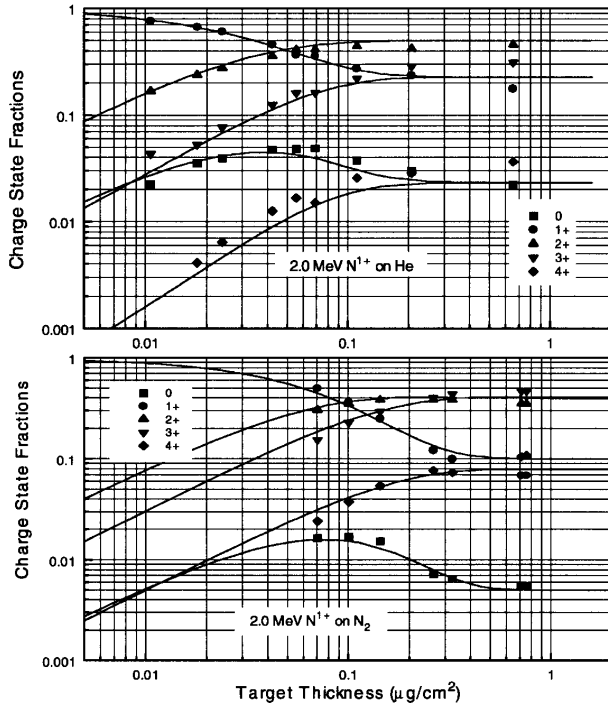


FIG. 1. Results of the measured charge state fractions obtained with a 2 MeV  $N^{1+}$  beam vs the He and  $N_2$  target thickness. A transition from a nonequilibrium to an equilibrium charge state is observed. The curves correspond to calculated charge state fractions as discussed in the text.

creased. At a target thickness of about 0.15 and  $0.40 \mu\text{g}/\text{cm}^2$  for helium and nitrogen, respectively, an equilibrium charge state distribution is achieved. Average equilibrium charge states  $\bar{q}$  of 2.2 and 2.6 have been obtained with helium and nitrogen targets, respectively. The lowest pressure obtainable in the gas cell was  $8.0 \times 10^{-4}$  Torr, which corresponds to a target thickness of about  $0.011 \mu\text{g}/\text{cm}^2$  air equivalent. When using the empty gas cell at this base pressure (without additional He or  $N_2$  gas), the  $1^+$  charge state fraction amounts to  $\sim 95\%$  of the beam intensity, demonstrating that the stripping effect of residual gas is negligible and that the incident beam is nearly pure.

The charge state distribution of the final beam is determined by the electron-capture and the electron-loss processes occurring in collisions between the ions (beam) and the target atoms. If the complete set of single and multiple charge-exchange cross sections is known, the charge state distribution at a given target thickness can be calculated.<sup>6,7</sup> The variation of the charge composition of an ion beam within a gas target is described by a system of linear coupled differential equations:

$$\frac{d\Psi_q(x)}{dx} = n \sum_{q' \neq q} \sigma(q', q) \Psi_{q'}(x) - \sigma(q, q') \Psi_q(x), \quad (1)$$

where  $\Psi_q$  denotes the fraction of ions with charge  $q$ ,  $x$  is the target thickness,  $n$  the target density, and  $\sigma(q, q')$  represents the cross section for charge exchange from  $q$  to  $q'$ .<sup>7</sup> Cross sections for electron loss and electron capture of nitrogen in various gases have been measured at different energies<sup>8-11</sup> and an interpolation of these data resulted in a complete set of charge-exchanging cross sections for 2 MeV nitrogen in

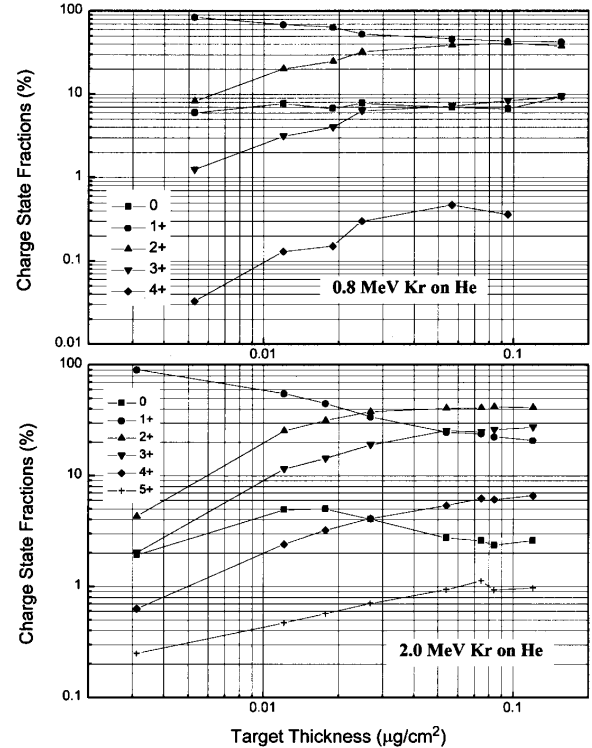


FIG. 2. Krypton charge state fractions vs the helium target thickness, measured at 0.8 and 2.0 MeV. Data points are connected to guide the eye.

helium and nitrogen gas. The curves in Fig. 1 are the calculated charge state fractions [numerical solution of (1)] taking into account single and double electron loss and capture cross sections (for the  $1^+$  charge state also a triple electron loss process is added) and using an effective thickness (see below). These calculations show a qualitative agreement with the experimental data, supporting a simple mathematical description of the nonequilibrium charge state distribution for ions stripped in dilute gases.

Because of the unknown gas profile outside the window-less cell, the effective target thickness is not well determined. However, comparison of the experimental data and the calculated charge state fractions provides a determination of this effective target thickness, independently of the cell pressure measurement and the target geometry. The difference between the target thickness obtained from the comparison of the experimental data with the theoretical curves and the thickness obtained from the pressure measurement, amounts to 8% and 24% for nitrogen and helium, respectively. An average target thickness, based on the two methods for obtaining the target thickness of the gas cell, has been adopted for the measurements with Kr, Xe, and Pb beams, as discussed below. The estimated uncertainty on the target thickness, obtained in this way, is of the order of 5% and 15% for nitrogen and helium targets, respectively.

## 2. Krypton, xenon, and lead results

The Kr, Xe, and Pb charge state distributions obtained with helium as a stripper gas are shown in Figs. 2, 3, and 4, respectively. Again, a transition from a nonequilibrium to an equilibrium charge state distribution is observed when going

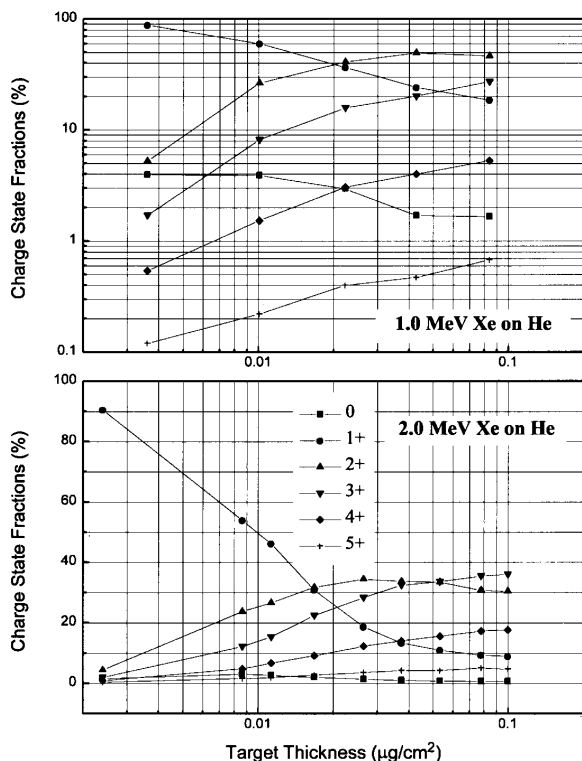


FIG. 3. Xenon charge state fractions vs the helium target thickness, measured at 1.0 and 2.0 MeV. Data points are connected to guide the eye.

from a low to a high target density. As shown, high  $1^+ - 2^+$  stripping efficiencies of 40%, 49%, and 50% are obtained for 0.8 MeV  $\text{Kr}^+$ , 1.0 MeV  $\text{Xe}^+$ , and 1.0 MeV  $\text{Pb}^+$ , respectively. When using 1.50 MeV and 1.82 MeV Pb beams, a  $1^+ - 3^+$  stripping efficiency of 40% and 45%, respectively, has been measured (Fig. 4). Notice also that the optimum  $2^+$  efficiency is not always obtained at the equilibrium thickness, as shown in Figs. 3 and 4. At higher energies, the  $2^+$  and  $3^+$  curves even cross and a maximum for the  $2^+$  charge state is obtained at a nonequilibrium target thickness as demonstrated with the 2.00 MeV  $\text{Xe}^+$  and 1.82 MeV  $\text{Pb}^+$  results. Figure 5 shows the Kr (0.8 MeV), Xe (1.0 MeV), and Pb (1.0 MeV) charge fractions obtained with nitrogen as a stripper gas. In all three cases, lower stripping efficiencies are obtained with nitrogen. The average equilibrium charge state fractions  $\bar{q}$  for Kr (0.8 MeV), Xe (1.0 MeV), and Pb (1.0 MeV) are 1.28, 1.67, and 1.53, respectively. Whereas the average fractions  $\bar{q}$  when using a He target correspond to 1.51, 2.18, and 2.23, respectively. Notice the large fraction of ions maintained in the initial  $1^+$  charge state (Fig. 5). The exceptionally high average equilibrium charge  $\bar{q}$  obtained with helium, compared to other gases, has been observed by several authors, provided that the ion velocity is low (see Ref. 7, and references therein). This anomalous effect of helium can be understood in view of the exceptionally high first ionization potential compared to other gases. This results in lower electron capture cross sections and, consequently, higher charge states for slow ions in helium.<sup>7</sup> The higher yields of  $2^+$  and  $3^+$  charge states when using helium make it the gas of choice for the proposed radioactive beam accelerator.<sup>1</sup>

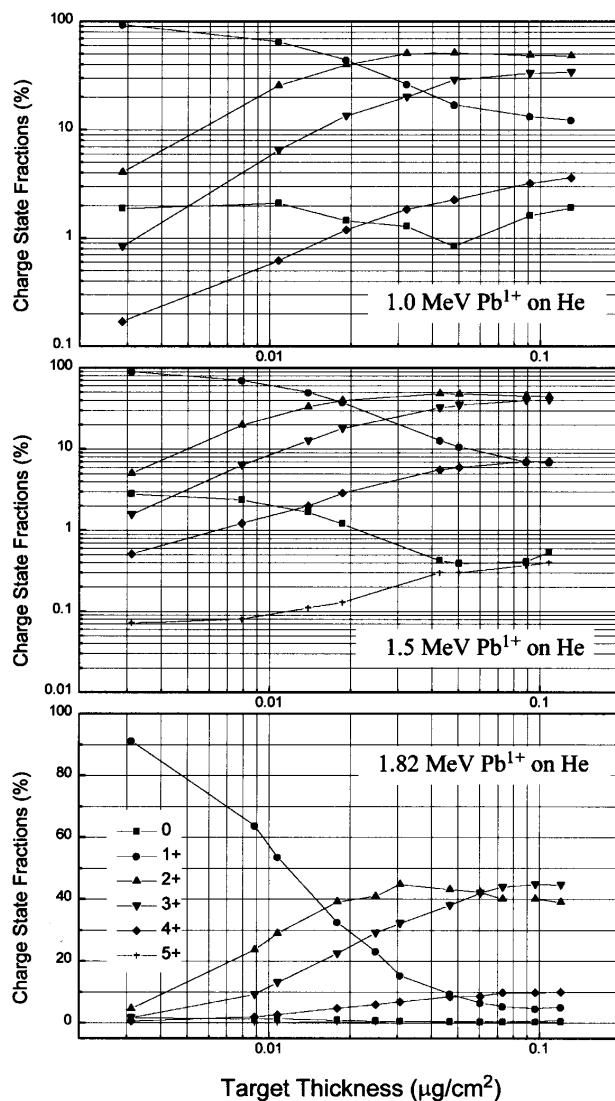


FIG. 4. Lead charge state fractions vs the helium target thickness, measured at 1.0, 1.5, and 1.82 MeV. Data points are connected to guide the eye.

### 3. Equilibrium charge state distributions

In view of the large range of ion species to be accelerated at an ISOL-based radioactive beam facility, information on stripping efficiencies for heavy ions with a low fixed velocity ( $v/c \approx 0.005$ ), and with atomic numbers in the broad range  $28 < Z < 92$  are of interest. Unfortunately, no quantitative theory is available to predict charge states of heavy ions in collisions with target atoms in gases. On the basis of general experimentally observed regularities, empirical relations have been deduced to predict average equilibrium charges and average distribution widths for specific velocity ranges and target species.<sup>7</sup> In particular, under equilibrium conditions when the final charge states are determined by competition of many charge-changing processes, the final charge can be represented as a sum of  $\nu$  independent variables and, consequently, follows a  $\chi^2$  law with  $\nu$  degrees of freedom. For large  $\nu$ , the central limit theorem implies a Gaussian normal distribution.<sup>12</sup> Equilibrium charge state distributions obtained in helium show a remarkable symmetry and can be described by a Gaussian distribution,<sup>7</sup> which is demonstrated

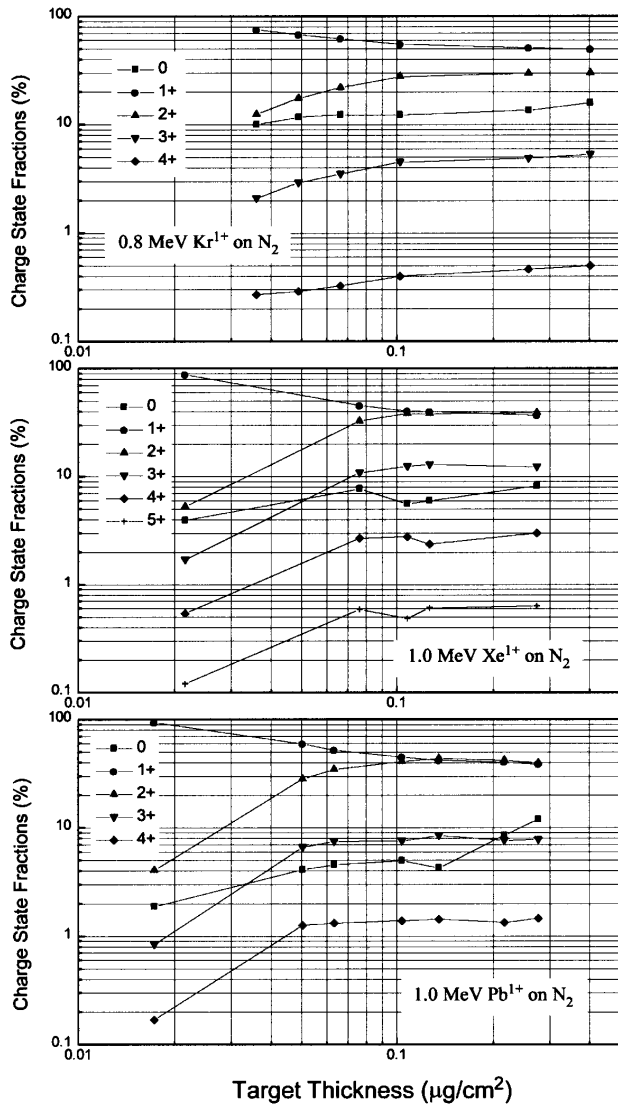


FIG. 5. Measured Kr (0.8 MeV), Xe (1.0 MeV), and Pb (1.0 MeV) charge state fractions vs the nitrogen target thickness. Data points are connected to guide the eye.

in Fig. 6 where the present results are shown together with a Gaussian fit. Hence, when the average charge state and the variance are known, the charge state distribution can be estimated. However, so far no predictions for low-velocity heavy ion stripping have been reported. We have now empirically deduced an analytical expression for the equilibrium average charges and the distribution widths for low-velocity ions in helium, based on all existing experimental stripping data at low energies. Following the theory on equilibrium charge states as discussed in Ref. 6, the relative equilibrium ionization ( $\bar{q}/Z$ ) is plotted versus the reduced velocity  $v_r = v/(v_0 Z^{2/3})$  ( $v$  is the ion velocity,  $v_0$  is the Bohr velocity  $= 2.188 \times 10^8$  cm/s, and  $Z$  the nuclear charge) in Fig. 7. All available experimental helium stripping data for ions with energies ranging between 0.8 and 2.0 MeV and  $17 < Z < 92$  have been used (present data and Ref. 13). The relative ionization may be approximated by a linear relation

$$\bar{q}/Z = 0.563v_r + 0.0139. \quad (2)$$

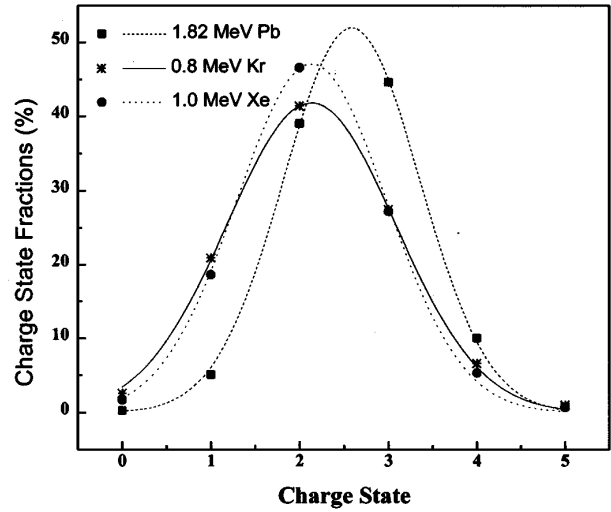


FIG. 6. Measured equilibrium charge state fractions for Pb (1.82 MeV), Kr (0.8 MeV), and Xe (1.0 MeV). The fitted curves shown represent Gaussian distributions.

With this expression, all experimental average charges can be described within 10%. Only the uranium data, which have a remarkably high average charge state, are underestimated. A second empirical expression has been deduced for the variances of the distributions. All experimental equilibrium charge state distributions (present data and Ref. 13), have been fitted with a Gaussian distribution. The  $2\sigma$  values ob-

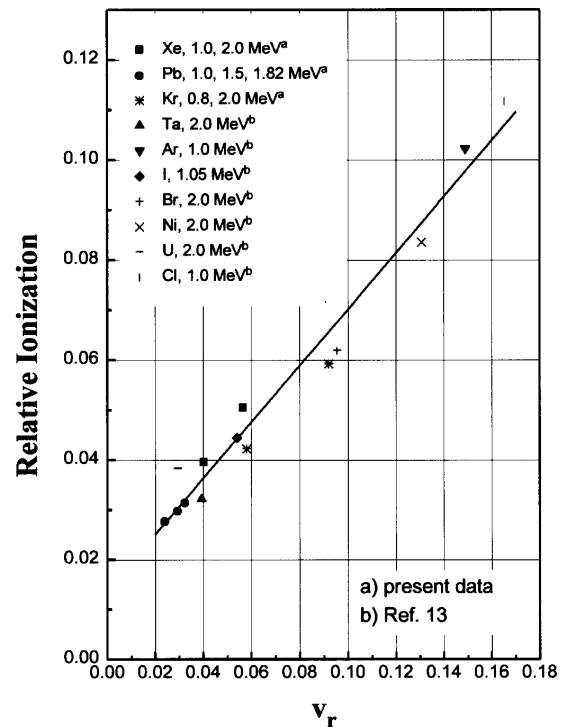


FIG. 7. Relative ionization  $\bar{q}/Z$  vs the reduced velocity. The data include present data and data taken from Ref. 13 (energy range: 0.8–2.0 MeV). A linear approximation has been made to the data points.

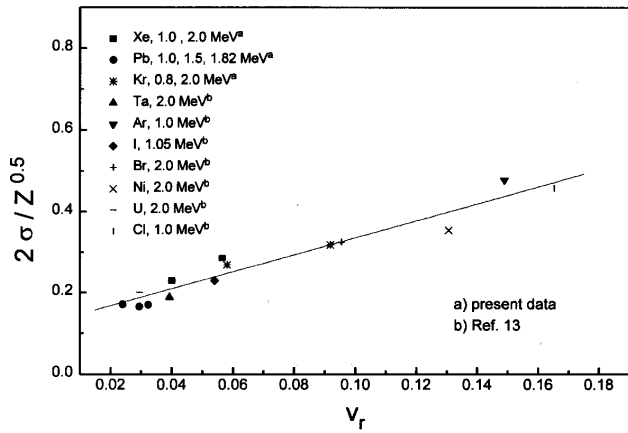


FIG. 8. Distribution width ( $2\sigma/Z^{1/2}$ ) versus the reduced velocity. The experimental points include present data and data taken from Ref. 13 (energy range: 0.8–2.0 MeV). A linear approximation has been made to the data.

tained range between 1.5 and 2.0. By plotting ( $2\sigma/Z^{1/2}$ ) versus the reduced velocity  $v_r$ , we find that a linear relation can approximate the experimental data (Fig. 8)

$$2\sigma/Z^{1/2} = 2.097v_r + 0.125. \quad (3)$$

Adopting a Gaussian charge distribution and by using the expressions (2) and (3), the equilibrium charge state distribution for heavy ions ( $28 < Z < 92$ ) has been estimated for three fixed ion velocities of  $v/c = 0.0040$ ,  $0.0050$ , and  $0.0060$ , as shown in Fig. 9. These calculations show that for a large range of elements, high  $1^+$  to  $2^+$  and  $1^+$  to  $3^+$  stripping yields are achievable in this velocity range. An optimum velocity has to be chosen in order to obtain the best overall efficiency, i.e., high  $2^+$ ,  $3^+$ , and  $4^+$  stripping yields for masses above 70, 140, and 210, respectively. Although atomic shell effects might affect charge-changing cross sec-

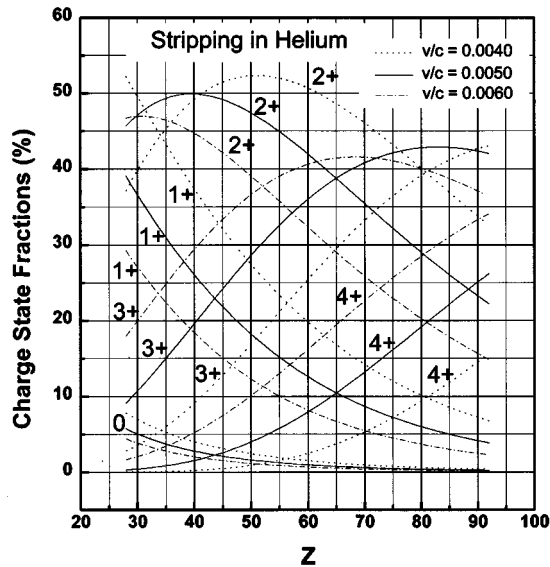


FIG. 9. Equilibrium charge state distribution for heavy ions ( $28 < Z < 92$ ), calculated for three fixed ion velocities of  $v/c = 0.0040$ ,  $v/c = 0.0050$ , and  $v/c = 0.0060$ . A Gaussian distribution is adopted and the average charges and the distribution widths are determined from Figs. 7 and 8, respectively [expressions (2) and (3)].

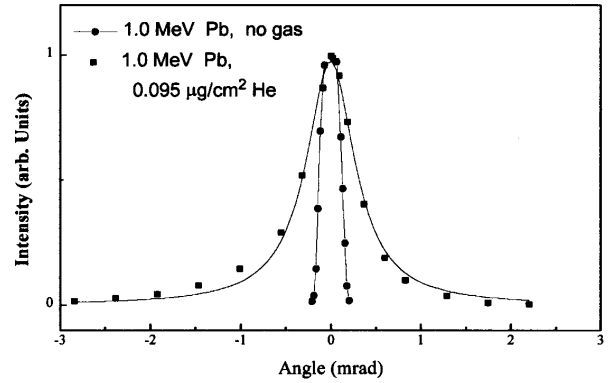


FIG. 10. Angular distribution of a 1.0 MeV Pb beam after passing a  $0.095 \mu\text{g}/\text{cm}^2$  He target. Also shown is the measured angular distribution of a 1.0 MeV Pb beam when no gas is added to the gas cell, in which case the width of the peak is determined by the resolution of the detection system (i.e.,  $\approx 0.2$  mrad).

tions and, hence, charge state distributions, the results of the present calculations, based on the deduction of expressions for the average charge and the distribution width, seem reliable within 20% for the charge fractions close to  $\bar{q}$ . Due to possible deviations from the Gaussian shape (e.g., due to influences from atomic shell effects), predictions of charge fractions further away from the average charge fraction  $\bar{q}$  are risky. Again the results of the calculations presented in Fig. 9 have to be interpreted as a guideline for the overall expected stripping efficiency (i.e., the most probable charge fraction) for a large range of elements.

## B. Multiple scattering

The small-angle multiple scattering for 1.0 MeV Xe and 1.0 MeV Pb beams in helium and nitrogen targets has also been measured. The multiple-scattering widths are obtained

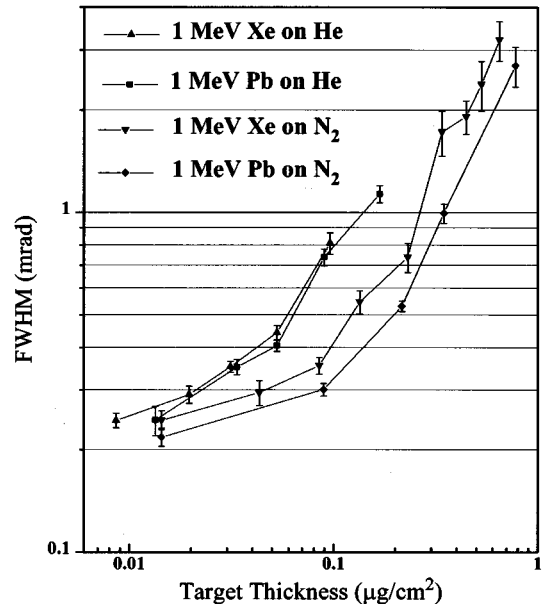


FIG. 11. The full width at half-maximum (FWHM) of the angular distributions of a 1.0 MeV Xe and Pb beam after passing a helium and a nitrogen stripping target (all charge states).

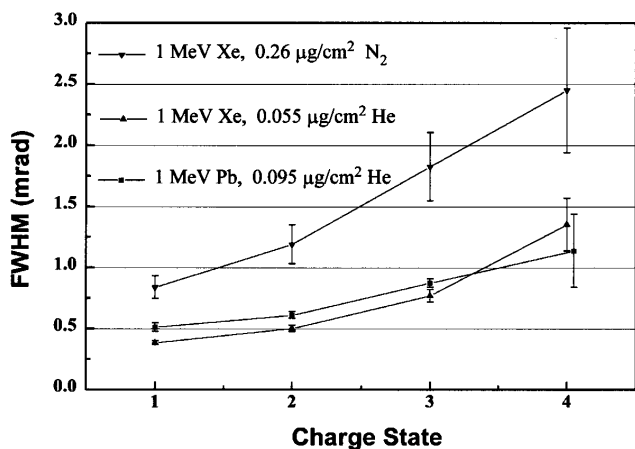


FIG. 12. The FWHM of the measured angular distributions of the  $1^+$ ,  $2^+$ ,  $3^+$ , and  $4^+$  charge state fractions, showing an increase of the width for higher charge states.

by scanning the outgoing beam with a movable silicon detector collimated to 0.2 mrad, as explained in Sec. II. Figure 10 shows an example of the angular distribution of a 1.0 MeV Pb beam after passing through a  $0.095 \mu\text{g}/\text{cm}^2$  He target. The angular distribution can well be described by a Lorentz curve. The distribution obtained when no gas is added to the target is also shown and reflects the resolution of the detection system. The full widths at half-maximum (FWHM) of the angular distributions of a 1.0 MeV Xe and a 1.0 MeV Pb beam after passing a helium and a nitrogen stripping target (all charge states) are plotted in Fig. 11. At target thicknesses adequate for obtaining high  $2^+$  and  $3^+$  stripping efficiencies, i.e., at nonequilibrium or near-equilibrium thicknesses (see Sec. III 2), the effect of the multiple scattering is small and remains below 1 mrad. When the target thickness is further increased, i.e., above the equilibrium thickness, the widths become significantly larger. The dependency of the widths on the final charge state has also been measured and is shown in Fig. 12. Because of the correlation between the ionization probability and the impact parameter, an enhancement of the widths with increasing charge state is observed, which is characteristic for single small-impact-parameter collisions and is expected to occur at nonequilibrium target thicknesses.<sup>14</sup> In view of the planned low-energy stripping of radioactive ion beams,<sup>1</sup> these results show that the use of He gas targets, at thicknesses adequate for obtaining high  $2^+$  and  $3^+$  stripping yields, are ideal for maintaining excellent-quality secondary beams. Helium is preferred over nitrogen as the stripping medium in this application due to the higher intensity as discussed above.

#### IV. DISCUSSION

Our results show that as much as 40%–50% of the beam can be stripped into the  $2^+$  charge state. Stripping into the  $3^+$  charge state with an efficiency of 45% has been obtained with a 1.82 MeV Pb beam. The high  $2^+$  and  $3^+$  yields

are the results of the narrow charge state distributions, obtained at these low velocities, combined with the relatively large  $\bar{q}$  achieved in helium gas. Approximate calculations of the equilibrium charge state distribution for low-velocity ( $v/c = 0.0040$ – $0.0060$ ) heavy ions in collisions with helium atoms, predict high  $2^+$  and  $3^+$  charge fractions for a large range of elements ( $28 < Z < 92$ ). The experimental stripping results also show that the effects of multiple scattering for target thicknesses smaller than or equal to that for reaching the equilibrium charge state distribution are small ( $\text{FWHM} \leq 1$  mrad). The results presented in this work are important in view of the postacceleration of radioactive ion beams, using linear accelerators. Our results demonstrate that low-energy ( $\approx 8$  keV/nucleon) stripping of radioactive beams from  $1^+$  to  $2^+$  and from  $1^+$  to  $3^+$  for masses higher than 70 and 140, respectively, is achievable with a high efficiency while maintaining the excellent beam quality of secondary beams. With this low-velocity stripping scenario, an overall gain of a factor of 2 in radioactive beam intensity is obtained when compared to high-velocity stripping scenarios (e.g., Iso-Spin Laboratory proposal,  $\approx 150$  keV/nucleon), where typical yields of 20% are achievable. Such stripping at higher velocities does reduce the total voltage required for the linac,<sup>15</sup> but this is at the expense of secondary beam intensity as mentioned above.

#### ACKNOWLEDGMENTS

This research was supported by the U.S. DOE Nuclear Physics Division under Contract No. W-31-109-ENG-38. The authors would like to thank A. Ruthenberg and K. Beyer for their technical assistance at the Dynamitron Facility.

- <sup>1</sup>Concept for an advanced Exotic Beam Facility, Internal Report, Physics Division, Argonne National Laboratory, February 1995, see also J. A. Nolen, and K. W. Shepard and J. W. Kim, *Proceedings of the 1995 Particle Accelerator Conference, Dallas, Texas, May 1–5* (IEEE, New York, 1995), pp. 354 and 1128.
- <sup>2</sup>J. A. Nolen, *Rev. Sci. Instrum.* **67**, 935 (1996).
- <sup>3</sup>P. Decrock, *Proceedings of the International Conference on the Application of Accelerators in Research and Industry*, edited by J. L. Duggan and I. L. Morgan, Denton, November 6–9, 1996 (to be published).
- <sup>4</sup>S. Chattopadhyay, *Part. Accel.* **47**, 119 (1994).
- <sup>5</sup>E. P. Kanter, P. J. Cooney, D. S. Gemmell, K. O. Groeneveld, W. J. Pietsch, A. J. Ratkowski, Z. Vager, and B. J. Zabranski, *Phys. Rev. A* **20**, 834 (1979).
- <sup>6</sup>S. K. Allison, *Rev. Mod. Phys.* **30**, 1137 (1958).
- <sup>7</sup>H. D. Betz, *Rev. Mod. Phys.* **44**, 465 (1972).
- <sup>8</sup>V. S. Nikolaev, I. S. Dmitriev, L. N. Fateeva, and Ya. A. Teplova, *Sov. Phys. JETP* **13**, 695 (1961).
- <sup>9</sup>V. S. Nikolaev, L. N. Fateeva, I. S. Dmitriev, and Ya. A. Teplova, *Sov. Phys. JETP* **14**, 67 (1962).
- <sup>10</sup>I. S. Dmitriev, V. S. Nikolaev, L. N. Fateeva, and Ya. A. Teplova, *Sov. Phys. JETP* **15**, 11 (1962).
- <sup>11</sup>I. S. Dmitriev, V. S. Nikolaev, L. N. Fateeva, and Ya. A. Teplova, *Sov. Phys. JETP* **16**, 259 (1963).
- <sup>12</sup>Baudinet-Robinet, *Phys. Rev. A* **26**, 62 (1982).
- <sup>13</sup>A. B. Wittkower and H. D. Betz, *At. Data* **5**, 113 (1973).
- <sup>14</sup>E. P. Kanter, *Phys. Rev. A* **28**, 1401 (1983).
- <sup>15</sup>P. Bricault, TRIUMF Report No. TRI-DN-93-20 (1993).